pH and Reactive Oxygen Species-Sequential Responsive Nano-in-Micro Composite for Targeted Therapy of Inflammatory Bowel Disease

DOI: 10.1002/ ((please add manuscript number))
Article type: Full Paper

Reactive oxygen species-responsive nano-in-micro composite for targeted therapy of inflammatory bowel disease

Serena Bertoni, Zehua Liu, Alexandra Correia, João Pedro Martins, Antti Rahikkala, Flavia Fontana, Marianna Kemell, Dongfei Liu, Beatrice Albertini, Nadia Passerini, Wei Li*, Hélder A. Santos**

S. Bertoni, Dr. W. Li, Z. Liu, A. Correia, J. P. Martins, Dr. A. Rahikkala, F. Fontana, Dr. D. Liu, Prof. H. A. Santos
Drug Research Program, Division of Pharmaceutical Chemistry and Technology, Faculty of Pharmacy, University of Helsinki, Helsinki 00014, Finland
E-mail: wei.li@helsinki.fi, helder.santos@helsinki.fi

Dr. D. Liu, Prof. H. A. Santos
Helsinki Institute of Life Science (HiLIFE), University of Helsinki
Helsinki 00014, Finland

S. Bertoni, Prof. B. Albertini, Prof. N. Passerini
PharmTech Lab, Department of Pharmacy and BioTechnology, University of Bologna, Via S. Donato 19/2, Bologna 40127, Italy
E-mail: nadia.passerini@unibo.it

Dr. M. Kemell
Department of Chemistry, University of Helsinki, Helsinki 00014, Finland

Keywords: nanoparticles; microfluidics; ROS-responsive; oxidation-responsive; inflammatory bowel disease

Abstract

Oxidative stress and abnormally high levels of reactive oxygen species play an essential role in the pathogenesis and progression of inflammatory bowel disease (IBD). Oxidation-responsive nanoparticles (NPs) are formulated from a phenylboronic esters-modified dextran (OxiDEX) that degrades selectively in response to hydrogen peroxide (H_2O_2). OxiDEX NPs are coated with chitosan and encapsulated in a pH-sensitive polymer to produce nano-in-micro composites. The microparticles are spherical with homogeneous particle size (53 ± 3 μm) and maintain integrity at acidic pH, preventing the premature release of the NPs in simulated gastric conditions. The degradation of NPs is highly responsive to the level of H_2O_2, and the release of the loaded drug is sustained in the presence of physiologically relevant H_2O_2 concentrations. The presence of chitosan on the particles surface significantly enhances NPs stability in intestinal pH and their adhesion on the intestinal mucosa. Compared to a traditional enteric formulation, this formulation shows ten-fold decreased drug permeability across C2BBe1/HT29-MTX cell monolayer, implying that lower amount of drug would be absorbed to the blood stream and, therefore, limiting the undesired systemic side effects. Based on these results, the developed nano-in-micro composite containing OxiDEX NPs has great potential for selective drug delivery in IBD treatment.

1. Introduction

Stimuli-responsive materials can undergo chemical structure change in response to environmental stimuli, such as enzymes, light, pH, temperature, ionic strength and various chemical species.[1] Advances in polymer science have led to the development of several novel reactive oxygen species (ROS)-responsive materials in the last few years. For example, the introduction of arylboronic moieties to common polymers such as poly amino-esters,[2] polyesters,[3] cyclodextrins,[4] polycarbonates[5] and PEG-lipid conjugate[6] provides specific sensitivity towards hydrogen peroxide (H_2O_2), making these polymers very attractive for the development of oxidation-sensitive systems. Within this group, an oxidation-sensitive dextran (OxiDEX) can be prepared by a simple modification of the hydroxyl groups of dextran, resulting in a responsive and biocompatible material, thus very promising for biomedical applications. [7] Drug delivery systems based on ROS-responsive polymers can be applied for various therapeutic purposes, as they represent a promising smart delivery vehicle for pathological disorders characterized by ROS overproduction, including cancers and inflammatory diseases,[8] such as inflammatory bowel disease (IBD).

IBD is a chronic inflammation of the gastrointestinal (GI) tract[9] and the therapy is based on daily administration of high doses of aminosalicylates, antibiotics, corticosteroids, and immuno-suppressive agents. Traditional formulations for IBD present high inter-patient variability[10] and several side effects due to systemic drug absorption.[11,12] A disease-targeted strategy is desired for IBD treatment, because it allows to target the drug directly to the site of action (inflammation) and achieve a controlled drug release, minimizing the unspecific absorption and subsequent systemic adverse effects. Oxidative stress plays an essential role in the pathogenesis and progression of IBD,[13] and diseased sites present abnormally high ROS level, as confirmed by biopsies of tissues taken from IBD patients showing from 10- to 100-fold increase in mucosal ROS concentrations.[14,15] The unusually high concentrations of ROS localized at sites of intestinal inflammation can be exploited

as a selective feature to target the delivery system, and avoid the release of the drug in the healthy tissue.[16,17] Accordingly, we identified the excessive generation of ROS as a disease-specific triggering mechanism to design a responsive drug delivery system. Nano-sized delivery systems have been recognized as a promising strategy for IBD treatment, because of their preferential accumulation in the inflamed regions of the intestine.[18] Additionally, nanoparticles (NPs) provide the potential of tailoring drug properties, including solubility, stability, and release behavior and their surface can be easily modified in order to introduce targeting-ligands or adjust surface characteristics (e.g., surface charge or adhesive properties).

Therefore, considering the potential of recently synthesized ROS-responsive polymers and the advantages of nano-sized systems in IBD treatment, it is important to evaluate these biomaterial for the development of smart high-precision medicines. The aim of this research is the development of an advanced oral drug delivery system able to meet multiple demands: protection of the responsive NPs against harsh GI environments, prevention of premature drug release and achievement of targeted and efficient local drug delivery to the diseased sites with limited systemic absorption. For this purpose, we designed a nanoplatform based on OxiDEX NPs to achieve an oxidation-responsive drug delivery, externally modified with chitosan (CS), known for its mucoadhesive properties. Mucoadhesion can be an additional advantage for IBD targeting as it promotes better contact with the mucosal surface and reduces the clearance of nanocarriers when the intestinal motility is increased, which is common in IBD, helping to maintain high local concentration of drug.[19] Rifaximin (RIF), an intestine-specific antibiotic successfully used in inducing remission of IBD,[20,21] was chosen as model drug. NPs were then encapsulated by microfluidics in hydroxypropyl methylcellulose acetate succinate (HPMCAS), a pH-responsive polymer, to produce nano-in-micro structured particles[22,23]. The final composites were designed to protect the NPs from the harsh

conditions of the upper GI tract (*e.g.*, acid pH of the stomach) and to release them in the intestine, closer to the targeted site. Thereafter, upon triggering by abnormally elevated ROS levels, the OxiDEX NPs will selectively release RIF to the inflamed tissues.

In this study OxiDEX has been explored for the first time as ROS-responsive material to prepare nano-in-micro composites for the encapsulation and "on demand" delivery of RIF at sites of oxidative stress.

2. Results and discussion

2.1. Characterization of nanoparticles

A H_2O_2-responsive material (OxiDEX) was synthesized and used to prepare NPs, which were subsequently coated with CS. The NMR spectrum of OxiDEX (**Figure S1a)** and the NMR study of the polymer degradation after treatment with and without H_2O_2 (**Figure S1ab)** confirmed the successful synthesis of the polymer.[7] The preparation procedure of the particles is schematically shown in **Figure 1a**.

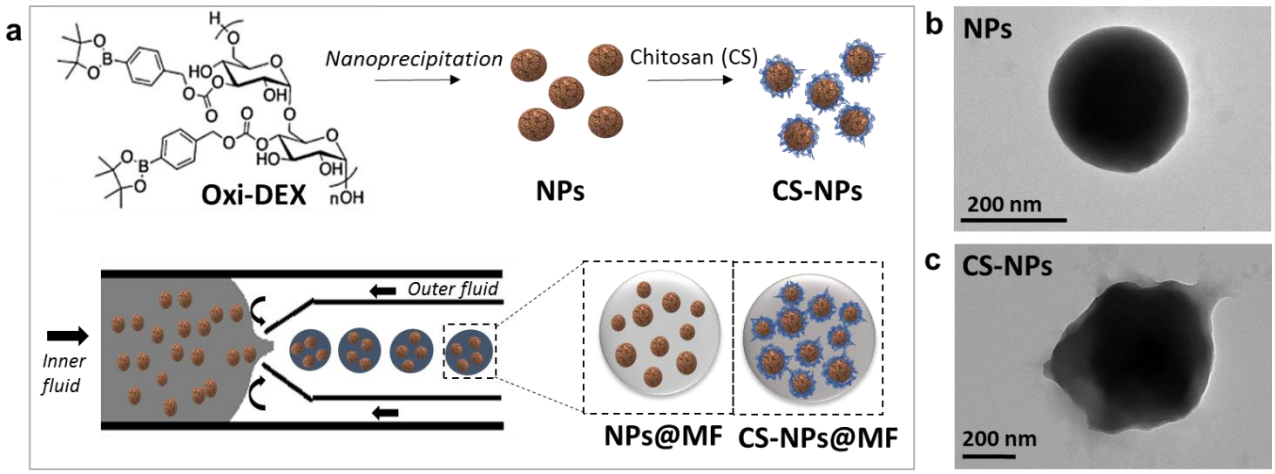

Figure 1. (a) Scheme of the production procedure of NPs and CS-NPs and schematic illustration of the fabrication process of the nano-in-micro composites by microfluidics: NPs and CS-NPs were encapsulated in MF grade of HPMCAS (MF) to form, respectively, the composites (NPs@MF and CS-NPs@MF). NPs or CS-NPs were dispersed in an ethyl acetate solution of MF, which served as inner oil fluid. The outer continuous fluid was 2% w/v P-407 aqueous solution (pH 4). TEM images of (b) NPs and (c) CS-NPs.

The size and polydispersity index (PDI) of OxiDEX NPs were firstly evaluated by dynamic light scattering (DLS). The hydrodynamic average size was 100-200 nm (**Figure 2a**), and it was not affected by the CS coating. Moreover, a relatively similar particle size distribution was observed for NPs and CS-NPs (**Figure S2**); however, a slightly wider particle size distribution was detected in the case of CS-NPs, due to the presence of CS layer on the particle surface, which led to a size distribution moved towards higher values and to an increased polydispersity. This trend was confirmed by a small increase in the PDI (**Figure 2a**), which passed from 0.303 to 0.363 after CS coating in the case of unloaded particles. Similarly, for RIF-loaded particles the PDI increased from 0.344 to 0.412 after CS coating. The presence of CS on the particle surface was confirmed by the measurement of zeta-potential, that changed from negative (−24.4 ± 1.7 mV) to positive (+11.6 ± 0.5 mV) (**Figure 2b**), because of the positively charged amino groups of CS. The morphology of OxiDEX particles was studied by transmission electron microscopy (TEM). TEM images of single particles (**Figure 1b,c**) and of multiple particles **(Figure S3**) show highly spherical particles in case of uncoated NPs, while a more irregular particle shape due to surface covering of CS was noticed for CS-NPs. The size of dried particles observed in TEM images was slightly larger than the average hydrodynamic diameter obtained from the DLS experiment, but still consistent with the DLS results if observing the size

distribution (**Figure S2**). Fourier transform infrared (FTIR) spectroscopy results are reported in **Figure 2c**. Dextran showed characteristic bands at 3400, 2923, and 915 cm^{-1}, attributed to O-H bonds, C−H bonds, and the α-glucopyranose ring, respectively.[24] After the boronic ester modification, we observed the presence of new bands at 1640, 1610 and 1540 cm^{-1} due to the C-H stretching vibrations of the aromatic groups. Moreover, after modification, the broad band at 3400 cm^{-1} due to dextran hydroxyl groups was markedly reduced and an extra strong band appeared at 1747 cm^{-1}, which can be related with the C=O stretching of the newly formed ester groups. These characteristic bands of OxiDEX can be found with minor shift in the NPs. Comparing the spectra of NPs before and after CS coating, in the CS-NPs extra bands (1541, 1560, 1653, 1676 and 1684 cm^{-1}) appeared, which were absent in the spectrum of NPs. In particular, the bands ranging from 1510 to 1650 cm^{-1} represent a distinctive feature of CS and may be attributed to its amide groups.[25] In this region, the two strongest signals (1676 and 1684 cm^{-1}) can be found in the spectrum of CS-NPs. In addition, compared to the FTIR spectrum of NPs, the carbonyl band (1650 cm^{-1}) was shifted to higher wavenumbers (1653 cm^{-1}) after CS coating. This strong band at 1653 cm^{-1}, which can be seen in the spectrum of pure CS, is characteristic of the polymer and attributed to the –C=O stretching vibration of its secondary amide.[25b,26]

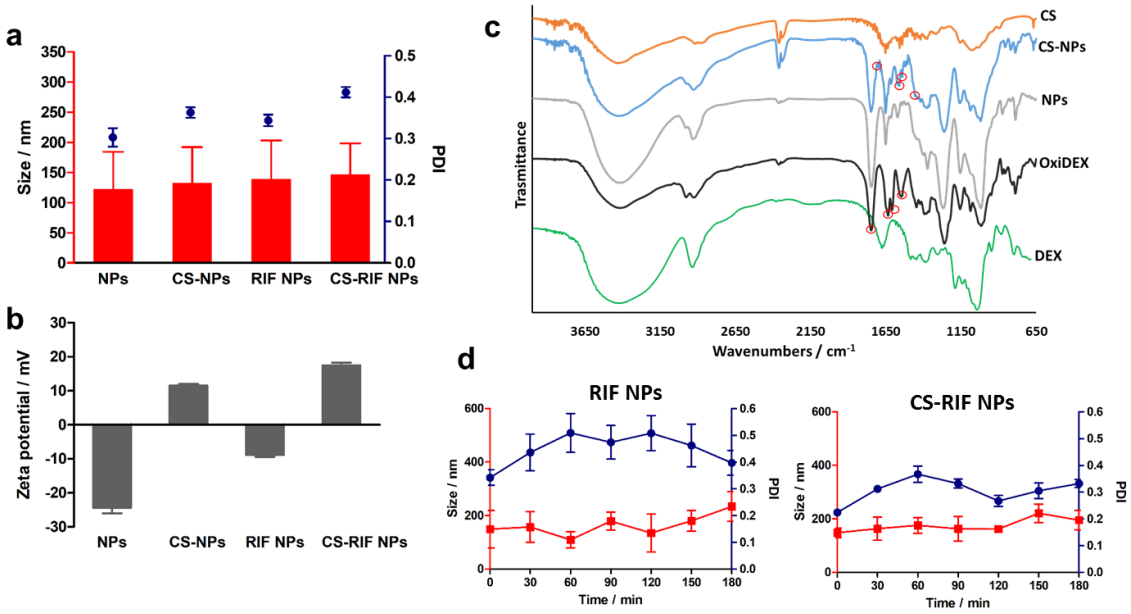

Figure 2. (a) Size and PDI and (b) zeta-potential of NPs and CS-NPs both unloaded and loaded with RIF. (c) FTIR spectra of dextran (DEX), OxiDEX, NPs, CS-NPs and pure CS. (d) Evolution of the nanoparticle size and polydispersity index (PDI) during incubation in simulated intestinal buffer. Data represent mean ± S.D. (n = 3).

The RIF loading in NPs was 3.3 ± 0.1% with an encapsulation efficiency of 6.6%; after CS coating, the drug loading was 2.9 ± 0.2%. Since the NPs are designed to deliver the drug locally on the intestinal membrane, the formulation needs to be stable the time necessary to reach the inflamed mucosa and to be degraded by the local ROS. Hence, the colloidal stability of RIF NPs and RIF CS-NPs was studied in a medium simulating intestinal conditions (**Figure 2d**). The average sizes of NPs showed fluctuations between 110 and 230 nm and the PDI, approximately 0.4, had also moderate variations. We found that the presence of CS on the NPs surface led to more stable particle size and lower PDI, which was around 0.3. Comparing these results with the ones obtained in MilliQ-water (**Figure 2a**) we can deduce that in the presence of saline buffer, the OxiDEX particles were less stable than in water. However, after CS coating, the stability in buffer increased significantly. In particular,

the average size was stable at 180 nm for the first 120 min, and only a small increasing in size (to around 200 nm) was observed in the third hour, suggesting that the NPs' tendency to aggregate in buffer was attenuated by the addition of CS coating.

2.2. H_2O_2-responsive degradation of NPs

The hydrolysis of OxiDEX NPs was examined in PBS containing various concentrations of H_2O_2, by measuring the amount of encapsulated drug released in the buffer after particle degradation (**Figure 3a**). Concentrations ranging from 0.1 to 1.0 mM of H_2O_2 were chosen basing on the sensitivity of OxiDEX, which had previously showed degradation when incubated with H_2O_2 1.0 mM.[7] In 1 h, more than 60% of RIF was released with 1.0 mM of H_2O_2 and even at low H_2O_2 concentration (100 µM), still more than 14% of the drug was released by the end of the test. NPs were not degraded in PBS alone (RIF released < 1% after 6 h). The appearance of NPs suspensions confirmed the H_2O_2 dependent degradation of the polymer: with increasing concentrations of H_2O_2, a yellow transparent solution can be observed, whereas a yellowish colloidal solutions could still be observed after 6 h of incubation in PBS (**Figure 3b**), indicating the presence of solid NPs. These results proved that degradation of OxiDEX NPs was highly responsive to the level of H_2O_2. In addition, TEM images of the NPs suspension in the 1.0 mM of H_2O_2 were taken at different time points to observe the evolution in the morphology of the NPs (**Figure 3c**). Already after 15 min, the NPs lost their original spherical shape, and some were swollen or partially degraded. This effect progressed overtime, showing a clear degradation of the particles after 60 min. OxiDEX is characterised by phenylboronic ester-groups, which might undergo hydrolysis in conditions of extreme pH.[27] For this reason, the physical stability of NPs was studied considering the physiological conditions of the GI tract (pH 1.2 for the gastric conditions and pH 6.8 for the intestinal environment, 37 °C). NPs showed a good physical stability

in pH 6.8, whereas a partial degradation was observed in highly acidic conditions (pH 1.2) (**Figure S4**).

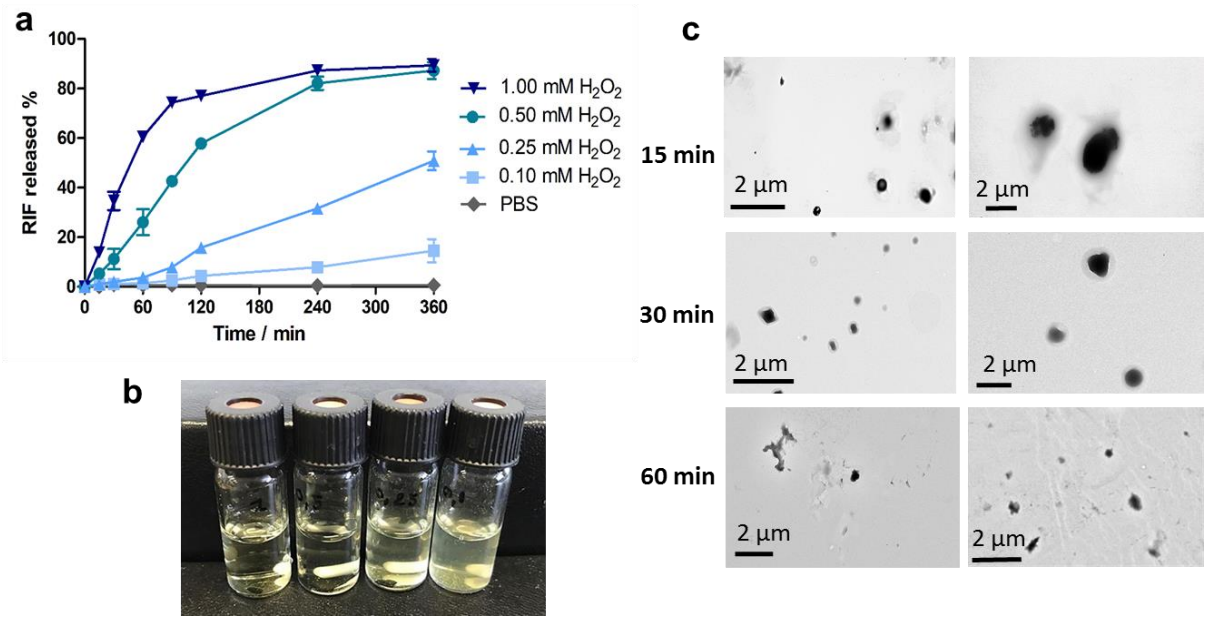

Figure 3. (a) RIF release from OxiDEX NPs in PBS buffers with various concentrations of H_2O_2. Data represent mean ± S.D. (n = 3). (b) Appearance of the suspensions of RIF NPs in buffers with 1.0, 0.5, 0.25 and 0.1 mM of H_2O_2 (from left to right). (c) TEM images of the RIF NPs suspension in 1.0 mM of H_2O_2 at different time points.

2.3. Characterization of nano-in-micro composites and *in vitro* drug release studies

RIF NPs and CS-RIF NPs were encapsulated in a pH-responsive polymer MF grade of HPMCAS (HPMCAS-MF)[28] to form nano-in-micro composites by microfluidics, named as RIF NPs@MF and CS-RIF NPs@MF, respectively. The preparation process is schematically illustrated in **Figure 1a**. This method allowed the production of microparticles with spherical shape (**Figure 4a**) and monodispersed particle size distribution, with prevalent size of 53 ± 3 µm (**Figure S5**). The distribution of NPs in the composites was studied by confocal microscopy (Figure 4a). To enable the visualization, NPs were labelled with fluorescein isothiocyanate (FITC) and the outer HPMCAS-MF

polymer layer was labelled with Nile red. Confocal images showed an efficient encapsulation of NPs in the composites. Moreover, the prevalence of yellow in the merged image indicated a co-localization of NPs and matrix, with a homogeneous distribution of the NPs within the polymeric matrix.

RIF NPs@MF and CS-RIF NPs@MF were immersed in simulated gastric fluid (SGF) at pH 1.2 and afterwards in PBS at pH 6.8 to evaluate the pH-responsive dissolution behaviour. As reported in **Figure 4b**, composites kept their integrity after 2 h immersion in pH 1.2, showing no change of morphology. Differently, microparticles started to lose their shape already after 5 min at pH 6.8, and they were completely degraded when the immersion time was prolonged to 2 h. These results suggest that nano-in-micro composites of based on HPMCAS-MF prepared by microfluidics are able to tolerate the harsh gastric conditions and to release the encapsulated NPs only at the typical intestinal pH (6.8).

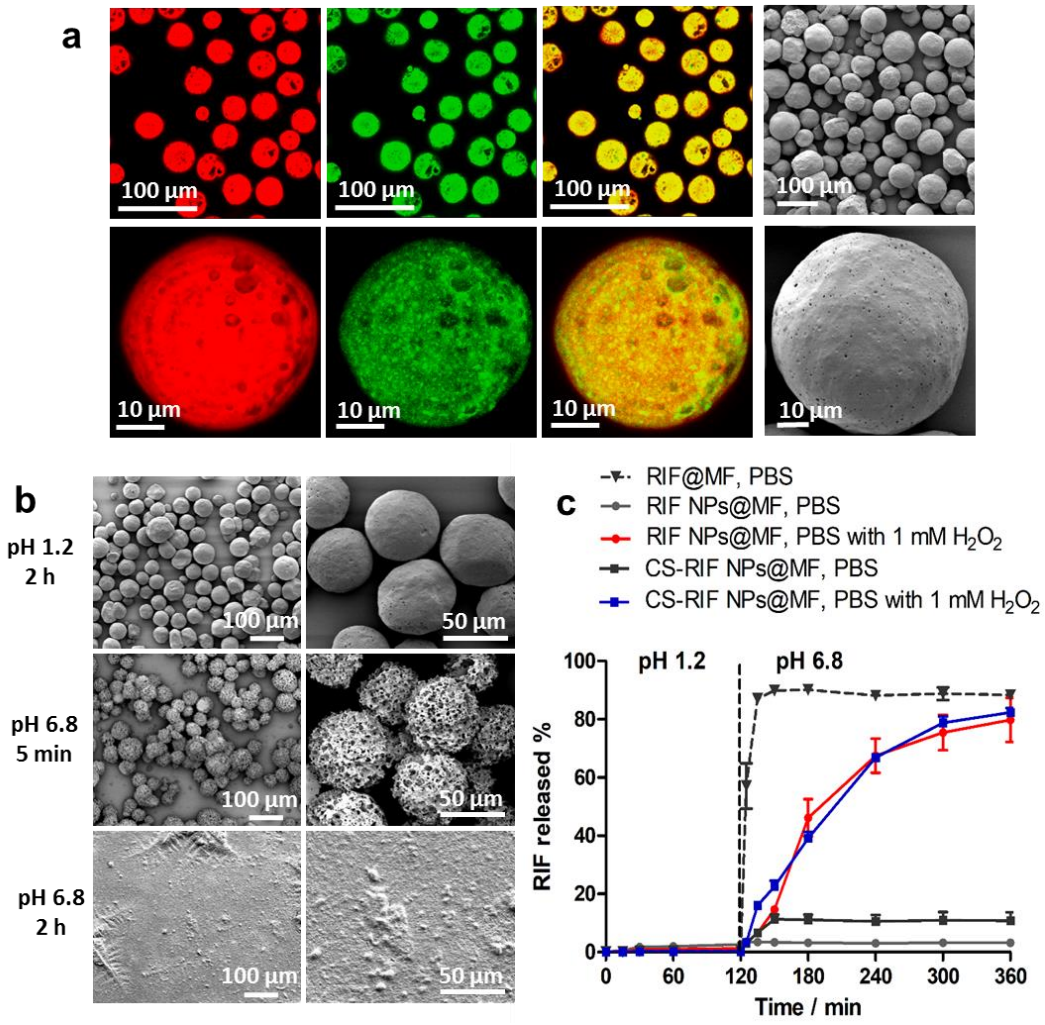

Figure 4. (a) FITC-labelled NPs were encapsulated in HPMCAS-MF with the addition of Nile red. The confocal images showed (from left to right) the Nile red, FITC and the overlay channels. In addition, the surface of the particles was observed by scanning electron microscope (SEM). (b) SEM images of RIF NPs@MF after immersion in SGF (pH 1.2) for 2 h, and in PBS (pH 6.8) for 5 min and 2 h. (c) Drug release profiles of nano-in-micro composites (RIF NPs@MF and CS-RIF NPs@MF) and reference formulation consisted of pure drug encapsulated in HPMCAS MF (RIF@MF) first in SGF (pH 1.2) for 2 h and then in PBS (pH 6.8) with or without H_2O_2 for 6 h. Data represent mean ± S.D. (n = 3).

In vitro drug release studies simulating the GI tract were carried out on the nano-in-micro composites (RIF NPs@MF and RIF CS-NPs@MF) and on a reference formulation, prepared by encapsulation of pure drug in the same enteric polymer HPMCAS-MF (RIF@MF), to better resemble the conventional commercial formulations. To evaluate the capability of the NPs to maintain the oxidation-responsive drug release after the encapsulation in the microcomposites, experiments in oxidative conditions (PBS with the addition of 1 mM of H_2O_2) were also performed. The release profiles (**Figure 4c**) showed that the MF matrix prevented the drug release at pH 1.2 in all samples. The release behaviour at pH 6.8 showed important differences: the drug was released immediately in the case of RIF@MF, while the RIF encapsulated in OxiDEX NPs was gradually released over 4 h. A controlled drug release is highly desired in IBD treatment, because it represents an advantage in terms of achieving the effective concentration required for local action and maintaining it over a sustained period of time. As expected, a very low drug amount (<10%) was released by the microcomposites in normal PBS buffer. It was interesting to notice that the coating with chitosan did not affect the dissolution behaviour. Additionally, to investigate the benefits of the nano-in-micro composites, *in vitro* release study of RIF NPs and CS-RIF NPs were also performed (**Figure S6**). In accordance with the previous results, the instability of OxiDEX in acidic pH led to more than 30% of RIF released in the gastric pH. In the second part of the study, performed at intestinal pH, the H_2O_2-responsive property of NPs was maintained, and a progressive drug release was observed only in oxidative conditions. As expected, no significant amount of drug was released in normal PBS.

2.4. In vitro cytotoxicity studies

The cytocompatibility of fabricated nanoparticles and nano-in-micro composites was evaluated on human colon carcinoma Caco-2 clone (C2BBe1) and human colon adenocarcinoma (HT29-MTX) cell lines, representing the enterocytes and the mucus-producing goblet cells of the intestine,

respectively.[29] The time points 6 and 24 h were chosen for this study as they correspond to the typical time that the particles would travel in the small intestine and the whole GI tract,[19] respectively. Cytotoxicity results are shown in **Figure 5**. OxiDEX NPs demonstrated to be safe for cells, even at very high concentrations (2000 μg ml^{-1}), as cell viability was higher than 80% for both cell types for both time points, excluding the highest concentration of NPs incubated for 24 h with HT29-MTX cells. Compared to uncoated NPs, CS-NPs led to lower cell viability, probably because of the positive charge of the surface: however, the cell viability was still higher than 80% in all cases. Finally, the microcomposites showed the lowest viability. One possible explanation for this could be the very large amount of samples added in order to maintain fixed NPs concentration. Moreover, we should consider that in physiological conditions, HPMCAS would be solubilized (it is soluble at pH > 6), and consequently, it would be quickly eliminated by physiological clearance. Thus, in the case of the final microcomposites, the experimental conditions were not fully representative of the *in vivo* situation, because the polymer remained in contact with cells during the whole experiment.

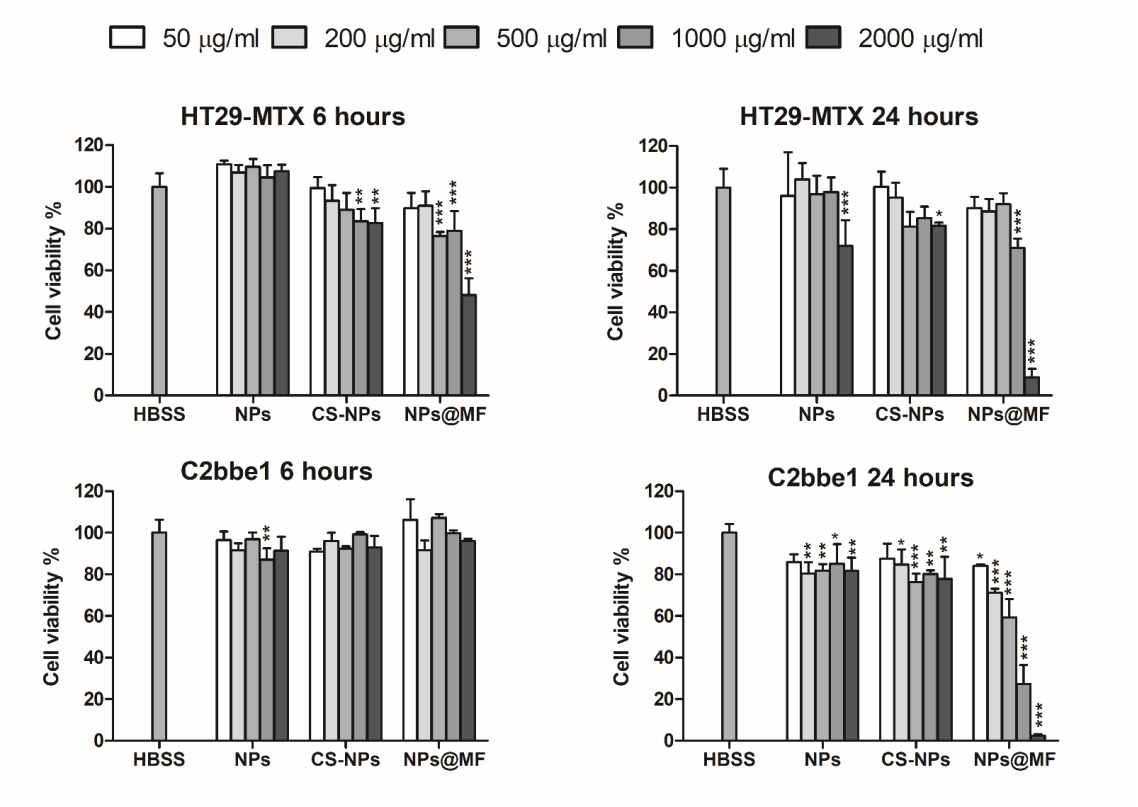

Figure 5. Viability of C2BBe1 and HT29-MTX cells after 6 and 24 h incubation with different concentration of NPs, CS-NPs, and nano-in-micro composites (NPs@MF). The concentration of NPs@MF was calculated based on the amount of encapsulated NPs. Data represent mean ± S.D. (n = 3), and the level of significance was set at the probabilities of $*p < 0.05$, $**p < 0.01$, and $***p < 0.001$ compared to the control (HBSS).

2.5. Study of cell monolayers in oxidative conditions

Preliminary tests showed that C2BBe1/HT29-MTX cell monolayers were responding in terms of increased ROS production to low concentrations (50 μM) of H_2O_2 and concentrations starting from 20 ng ml^{-1} of interleuchin-1β (IL-1β). Thus, they were used in combination to obtain monolayers in oxidative conditions. Treated monolayers exhibited higher ROS levels in the extracellular buffer, detected in the upper compartment, after 24 h incubation (**Figure S5b**), confirming the oxidative

stress state. These monolayers were then compared with non-treated ones in terms of membrane integrity and mucus layer characterization. IBD is reported to be associated with disruption of the intestinal epithelial layer, loss of barrier function and increased permeability.[30] Discordant data are reported regarding the mucus intestinal layer in IBD patients: increased mucus layer thickness was observed,[18] while dysregulated mucin production with loss of protective mucus layer was also reported.[31] In our cell model, the membrane integrity was slightly reduced in the oxidizing monolayers, as suggested by a modest, but still statistically significant drop in transepithelial electrical resistance (TEER) of 20–25% (**Figure 6a**). This result was similar to the one obtained by Leonard et al. after treatment with IL-1β.[32] Moreover, the result is also in accordance with the permeability studies, where the drug permeability was higher in simulated oxidative conditions.

The mucus layer distribution on C2BBe1/HT29-MTX cell monolayers was qualitatively studied by different staining methods. **Figure 6b** shows acid mucins stained by Alcian Blue, neutral and basic mucins colored by Periodic acid–Schiff (PAS) staining, and a combination of both methods. Mucins were distributed on the monolayers in an irregular layer. The morphology of the mucus layer was similar for the oxidative conditions as well as for the control. The quantitative analysis (**Figure 6c**) showed no statistical differences in mucin content between stimulated and non-stimulated monolayers. The results suggested that the external mucus layer was not altered in oxidative conditions. Therefore, the mucoadhesive properties of NPs may be exploited to achieve better contact with the mucosal surface even in the case of oxidative stress conditions.

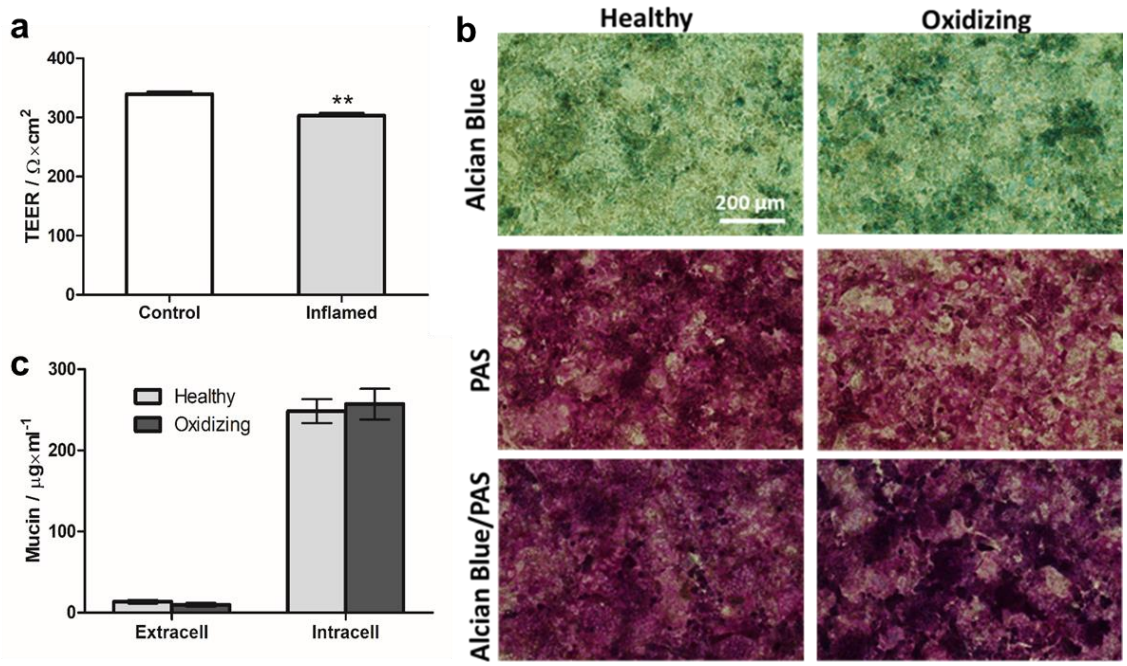

Figure 6. (a) Membrane integrity attested by TEER measurement of cell monolayers in healthy and oxidizing conditions. The level of significance was set as $^{**}p < 0.01$. (b) Qualitative mucus determination of cell monolayers in healthy and oxidative conditions. The scale bar is 200 µm for all images. (c) Mucus quantification in monolayers with periodic acid/Schiff stain colorimetric assay (mean ± SD, n = 3).

2.6. Mucoadhesion of the particles to C2BBe1/HT29-MTX cell monolayers

The interaction between NPs and intestinal cells was qualitatively studied by confocal laser scanning microscopy (CLSM). Wheat Germ Agglutinin-Alexa Fluor 594 conjugate (WGA-AF 594) was used to stain the mucus, as it binds to sialic acid and N-acetylglucosaminyl residues mainly localized in the mucus layer, which is particularly indicated when the objective is the evaluation of a mucoadhesive formulation.[24] As can be seen in **Figure 7**, CLSM images showed no or minimal interactions between cells and OxiDEX NPs. The particles appeared as green, suggesting only a superficial adhesion to the cell monolayer, but no strong interaction with the mucus layer. Differently,

for CS-coated NPs, more particles were observed on the cells. The larger amount of CS-NPs could be explained by the presence of CS on the NPs surface. The mucoadhesive properties of CS determined a high rate of interaction of CS-NPs with the co-cultured cells, thus decreasing the probability of washing away the particles during sample preparation. Electrostatic interactions of cationic CS with the negatively charged mucin are the main reason for CS strong mucosal adhesion.[33] Notably, most CS-NPs appeared as yellow, indicating a co-localization with the red-stained mucins of the mucus layer on the surface of the monolayer and, thus, a preferential accumulation of CS-NPs on the mucus layer on the intestinal membrane.

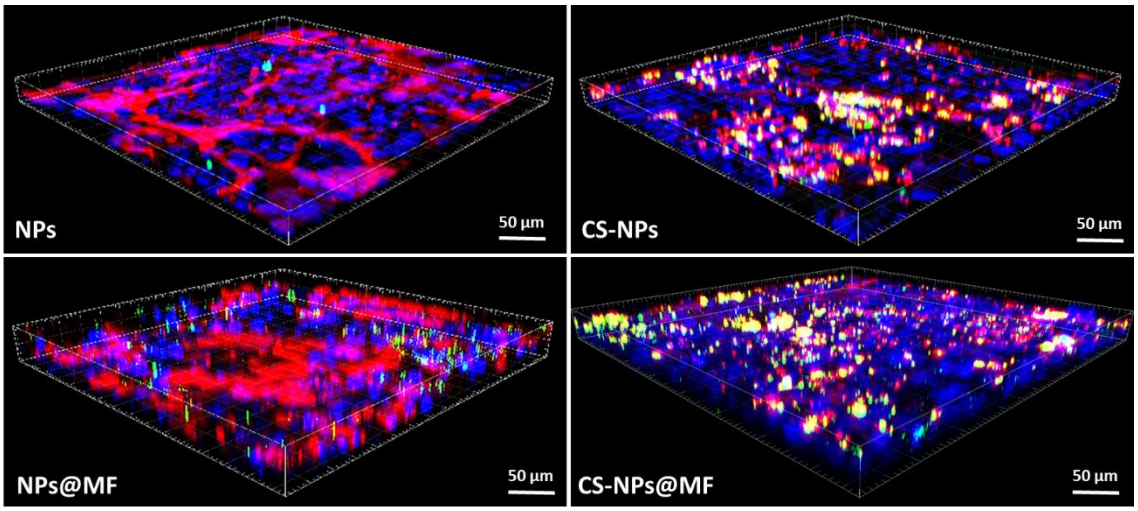

Figure 7. 3D Confocal microscope images of C2BBe1/HT29-MTX monolayers treated with NPs and CS-NPs (250 µg ml^{-1}) labelled with FITC after incubation with the cells at 37 °C for 4 h. Blue: cell nuclei stained with DAPI; Red: mucus layer stained with WGA-AF 594; green: FITC-labelled particles; and yellow: co-localization of NPs/CS-NPs and mucus.

2.7. Drug permeability across C2bbe1/HT29-MTX cell monolayer

After 21 days, the cell monolayers were completely differentiated and tight junction formed, as confirmed by TEER values stabilized at around 650 Ω.cm^2 (**Figure S5a**). This model closely mimics

the in vivo intestinal membrane.[34] Permeability curves and apparent permeability coefficients (P_{app}) are reported in **Figure 8a,b**, respectively. As observed from the permeation profiles, free RIF encapsulated in HPMCAS-MF showed the highest permeability, with a P_{app} of 5.41×10^{-6}. RIF encapsulated in NPs@MF and CS-NPs@MF had very low permeability (5.26×10^{-7} and 5.73×10^{-7}, respectively). The P_{app} values of RIF were significantly decreased after encapsulation into the OxiDEX NPs, indicating that the NPs were effective to limit the drug absorption through intestinal membrane and therefore decrease the drug amount in the systemic circulation.

Formulations were also tested with the addition of 1 mM of H_2O_2 in the donor compartment, to simulate an oxidative extracellular condition. This condition with high-oxidative medium allows a complete release of the drug after degradation of the H_2O_2-sensitive NPs. Comparing the P_{app} in the two conditions, the permeability resulted enhanced in the case of oxidative conditions for all samples. In particular, for RIF NPs@MF and CS-RIF NPs@MF, only in the presence of oxidizing species in the medium the drug was released and slowly permeated through the cell monolayer. The drug permeability was higher in oxidative conditions also in the case of RIF@MF, despite the absence of the H_2O_2-sentitive polymer, suggesting that the presence of H_2O_2 could influence the membrane integrity and contribute to increase drug permeation. Overall, the data indicate that the permeation of RIF may be drastically reduced by incorporation in OxiDEX NPs, especially in healthy conditions, representing an advantage in terms of unspecific absorption and systemic side effects.

After the permeability studies, the cell monolayers were observed under TEM (**Figure 8c,d**). The morphology of the cell monolayers was similar for all conditions, and the incubation with RIF NPs@MF and CS-RIF NPs@MF did not affect the appearance of the microvilli, indicating that the formulations have no toxic effects on the cell monolayers under the present experimental conditions tested. TEM images also showed some spherical dots (marked with red arrows) on the apical side of the monolayers near the microvilli, with dimensions quite similar to each other and in the range of

the actual NPs (size around 100 nm). In particular, the dots seemed to be mainly attached to the cell monolayers or to remain in the close vicinity of the microvilli. It can be clearly noticed that more dots are present in the sample with CS-NPs, compared to the one with NPs, suggesting that the CS coating influenced the adhesiveness of the particles and the interactions with cells, thus confirming the results from confocal microscopy.

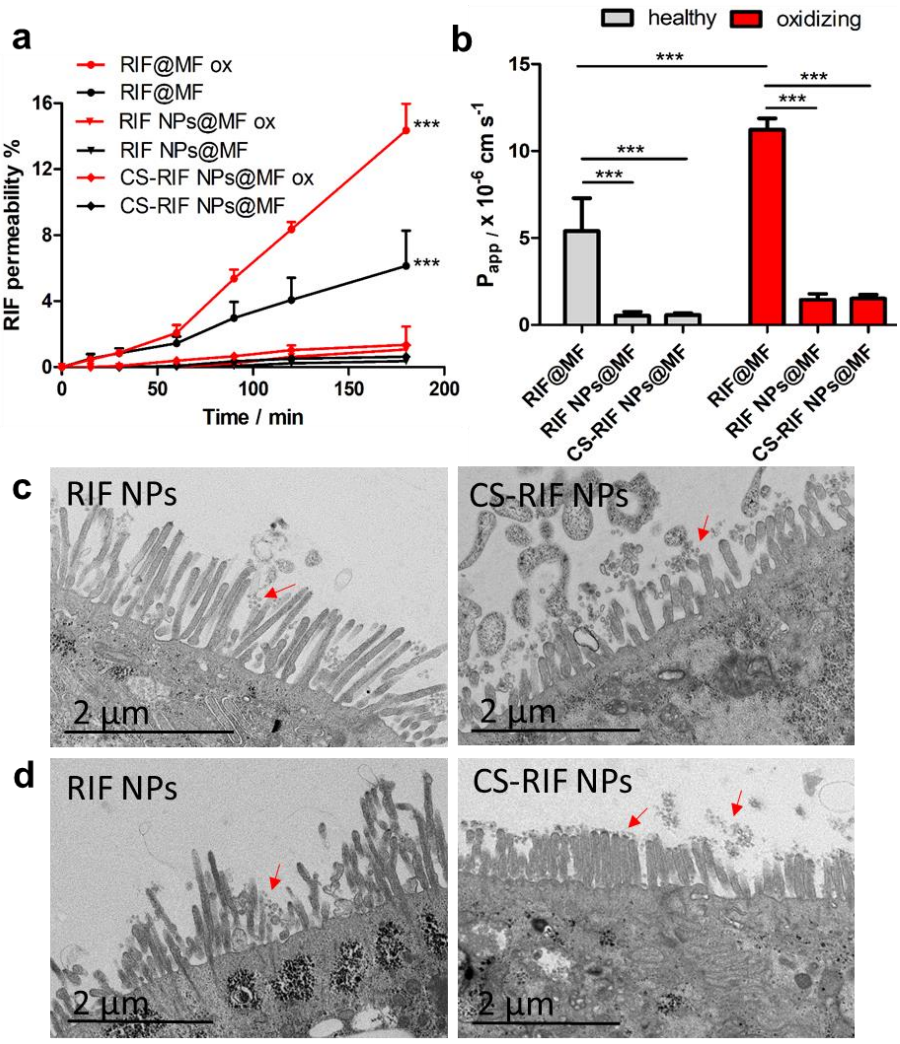

Figure 8. (a) Permeation profiles of RIF across co-cultured C2BBe1/HT29-MTX (ratio of 9:1) cell monolayers in normal or oxidizing (ox) conditions. The level of significance between the permeability of RIF@MF and the nano-in-micro composites (RIF NPs@MF and CS- RIF NPs@MF) in the same conditions were set at the probabilities of ***$p < 0.001$. (b) Apparent permeability

coefficient (P_{app}) of RIF calculated from the drug permeation profiles. Data represent mean ± S.D. (n = 3). The level of significance was set the probability of ***$p < 0.001$. TEM images of flat embedded sections of monolayers after permeability studies showing (c) RIF NPs and CS-RIF NPs interacting with the monolayers in healthy conditions and (d) with the monolayers simulating oxidizing conditions.

3. Conclusion

In this study, we developed nano-in-micro composites to achieve an oxidation-responsive delivery of RIF for IBD treatment. A phenylboronic esters-modified dextran (OxiDEX) was successfully employed to prepare RIF-loaded NPs, which showed highly H_2O_2-responsive degradation and controlled drug release in the presence of physiologically relevant (equal to or higher than 100 μM) H_2O_2 concentrations. The coating of NPs with CS significantly enhanced their stability in intestinal pH and their interactions with the intestinal mucosa, showing high mucoadhesive properties. Microfluidics allowed the encapsulation of NPs in HPMCAS, resulting in spherical and uniform microparticles able to protect the NPs from the harsh conditions of the stomach and to release them in the intestine. Compared to a traditional enteric formulation, the final composites showed ten times-decreased drug permeability across C2BBe1/HT29-MTX cell monolayer, indicating that OxiDEX NPs were effective to limit the drug permeation through intestinal epithelium, and therefore, representing an advantage in terms of unspecific absorption and systemic side effects. Overall, these results suggest that the prepared composite is a promising strategy for selective drug delivery in IBD treatment.

4. Experimental Section

Preparation of OxiDEX nanoparticles: An oxidation-responsive dextran-modified polymer (OxiDEX) was synthesized using the procedure of Broaders et al.[7] with minor modifications and characterized by NMR. More detailed information can be found in the **Supporting Information**. OxiDEX NPs were prepared by nanoprecipitation method. OxiDEX (5 mg) was dissolved in dimethylsulfoxide (DMSO) (0.25 ml), and then added dropwise into the anti-solvent (ethyl acetate, 2.5 ml) under magnetic stirring. The formed NPs were collected by centrifugation at 10000 rpm for 5 min washed with ethyl acetate and dried under vacuum at room temperature overnight.

Drug loading: RIF loaded nanoparticles (RIF NPs) were prepared using the method described above, but adding RIF (2.5 mg) in the OxiDEX solution. The concentration of RIF in samples was determined by Agilent 1100 high performance liquid chromatography (HPLC, Agilent Technologies, USA) with a mobile phase composed of phosphoric acid (0.1%, pH 3.3) and acetonitrile (volume ratio 50:50) at a flow rate of 1mL min^{-1}. A Gemini® 3 µm NX-C18 110 Å column (Phenomenex, USA) was used as stationary phase. The injection volume of the samples was 10 µl and the detection wavelength was 293 nm. For the drug loading determination, 1 mg of NPs was accurately weighed and stirred in a mixture of 0.1 M of H_2O_2 (0.5 ml) and acetonitrile (0.5 ml) for 2 h, until complete dissolution. The sample was centrifuged and the drug content in the supernatant was analyzed by HPLC.

Coating of nanoparticles with chitosan: After preparation, NPs were coated with CS by physical adsorption method.[35] Medium viscosity chitosan (Mw=190000-310000 Da, 75-85% deacetylated, Sigma-Aldrich, USA) was dissolved in 0.1 % acetic acid solution to obtain a 1% solution and the pH was adjusted to 5.5 by slowly adding sodium hydroxide solution. NPs and RIF-NPs were dispersed in 0.9 ml of MilliQ-water by sonication, 0.1 ml of CS solution was added to the NPs dispersion to have a final CS concentration of 0.1%. NPs were magnetically stirred with the CS solution for 1 h.

CS-NPs and RIF-loaded CS-coated NPs (CS-RIF NPs) were collected by centrifugation and washed with MilliQ-water.

Characterization of OxiDEX NPs: Size distribution and surface charge of NPs and RIF NPs before and after CS coating were determined by Zetasizer Nano ZS (Malvern Instruments Ltd, UK) in MilliQ-water (pH 7.4). Transmission electron microscopy (TEM; JEOL 1400, Japan) was used to observe the morphology of NPs before and during degradation study in presence of H_2O_2. TEM images were obtained with 80 kV acceleration voltage in bright-field mode. The chemical composition of dextran, OxiDEX, NPs, CS-NPs and pure CS was characterized by FTIR (Vertex 70, Bruker, USA). The FT-IR (KBr) spectra were recorded in the range of 4000–650 cm^{-1} with a resolution of 4 cm^{-1} using OPUS 5.5 software. Differential scanning calorimetry (DSC; AG-DSC823e, Mettler Toledo, Switzerland) was performed on OxiDEX, NPs, pure drug and physical mixture (PM). Samples were heated from 25 °C to 250 °C under nitrogen flow at a heating rate of 10 °C min^{-1}. Stability study was performed on drug loaded NPs and CS-NPs using Hanks' balanced salt solution (HBSS) as buffer to mimic the intestinal medium (pH 6.8).[36]

In vitro evaluation of oxidation-responsive degradation of the NPs: The response of OxiDEX NPs exposed to H_2O_2 and the consequent release of the drug were studied *in vitro*. RIF NPs (250 µg) were incubated in 1 ml of PBS buffer (pH 6.8, 37 °C) containing various concentrations (0, 0.1, 0.25, 0.5, 1.0 mM) of H_2O_2. At different time points, 100 µl of NPs suspension were withdrawn, centrifuged and the drug content in the supernatant was analyzed by HPLC. To study the stability of NPs in acidic conditions and the possible hydrolysis of NPs, quantitative experiments were conducted by measuring the absorbance of NPs-containing aqueous solutions (pH 1.2 and pH 6.8, 37°C) at 500 nm at various time points.

Microfluidic assembly of nano-in-micro composites: NPs were encapsulated by microfluidics in an enteric polymer, HPMCAS MF grade (HPMCAS-MF) with oil-in-water emulsion. The flow focusing

microfluidic chip consisted of two borosilicate glass capillaries (World Precision Instruments, USA) assembled on a glass slide, as described elsewhere.[37] The injection rates of the inner oil fluid (HPMCAS-MF 10 mg ml^{-1} in ethyl acetate) and the outer fluid (2% w/v Poloxamer 407 aqueous solution, pH 4) were 2 ml h^{-1} and 20 ml h^{-1}, respectively. RIF NPs and CS-RIF NPs were dispersed in the inner fluid before microfluidic process by tip sonication (weight ratio NPs:HPMCAS-MF 1:3). The formed droplets were collected in 1% Poloxamer 407 solution (pH 4.0). The solidified microparticles were collected by centrifugation, washed with MilliQ water (pH 4.0) and dried in a vacuum oven at 50 °C overnight. In addition to encapsulation of RIF NPs (NPs@MF) and CS-RIF NPs (CS-NPs@MF), free drug was encapsulated (RIF@MF) to obtain a reference formulation.

Labelling of nanoparticles with FITC: For confocal imaging, NPs were fluorescently labelled by loading of FITC. Briefly, FITC was added in the DMSO solution of the polymer to have a final concentration of OxiDEX and FITC of 20 mg ml^{-1} and 0.2 mg ml^{-1}, respectively (ratio FITC:OxiDEX 1:100). The obtained solution was used to prepare labelled NPs using the same nanoprecipitation method.

Characterization of nano-in-micro composites and in vitro drug release studies: To determine the distribution of the NPs into the microparticles of MF, CLSM was applied. FITC-labelled NPs were encapsulated in MF and Nile red was added as fluorescent dye to the inner fluid during the preparation of nano-in-micro composites. After microfluidic fabrication, the produced composites were arranged into 35 mm Petri-Dish with a thin bottom and imaged by CLSM (Leica SP5 II HCS A, Germany).

The release profiles of the nano-in-micro composites were evaluated by using pH variation method (pH 1.2 and pH 6.8), as described in the European Pharmacopoeia. NPs@MF, CS-NPs@MF (equivalent to 10 µg of RIF) were added to 1 ml of SGF (pH 1.2). After 2 h, particles were collected by centrifugation and resuspended in PBS buffer (pH 6.8) for additional 6 h. The test was conducted at 37°C with stirring at 100 rpm. At specific time points, 100 µl of the release medium were

withdrawn, centrifuged to remove the solid particles and the amount of drug in the supernatant was quantified by HPLC. 100 µl of fresh medium were added to keep the volume constant. The morphology of nano-in-micro composites before and during the release study was examined by scanning electron microscopy (SEM, Hitachi S-4800, Japan). To investigate the benefits of the nano-in-micro composites, release studies were performed also with RIF NPs and CS-NPs, following the same experimental procedure.

Cell culture: Human colon carcinoma Caco-2 clone C2BBe1 and human colon adenocarcinoma HT29-MTX were cultured in separate 75 cm^2 culture flasks in high glucose (4.5 g l^{-1}) Dulbecco's modified Eagle's medium (HyClone, Logan, UT) containing 10% of fetal bovine serum (Gibco, Invitrogen, USA), 1% (v/v) of L-glutamine, 1% (v/v) of nonessential amino acids, 100 IU ml^{-1} of penicillin, and 100 mg ml^{-1} of streptomycin (HyClone, Logan, UT). Cells were grown at 37°C in 5% of CO_2 and 95% relative humidity and the cell medium changed every other day.

In vitro cytotoxicity studies: Cytotoxicity of NPs, CS-NPs and nano-in-micro composites on cells was evaluated using CellTiter-Glo (Promega Corporation, USA). C2BBe1 and HT29-MTX were separately seeded in 96-well plates at a density of 2×10^5 cells per ml and left to attach for 24 h. Then, the medium was discarded and cells were washed with 100 µl of Hanks' balanced salt solution–4-(2-hydroxyethyl)-1-piperazinethanesulfonic acid (HBSS–HEPES, pH 7.4). Formulations were added to each well at a concentration of 50, 200, 500, 1000 and 2000 µg ml^{-1} (NPs or equivalent) and incubated for 6 and 24 h. Afterwards, cells were washed twice with HBSS–HEPES and the number of viable cells was quantified by addition of CellTiter-Glo. Luminescence was measured using a Varioskan Flash plate reader (Thermo Fisher Scientific, USA). HBSS–HEPES without particles and Triton X-100 1% were used as negative and positive control, respectively.

Study of cell monolayers in oxidative conditions: Altered intestinal barrier integrity and significant modifications in mucus layer structure are typical in IBD active inflamed sites.[19] Therefore, monolayers in healthy and oxidative stress conditions were studied in terms of membrane integrity and mucus layer amount and distribution, after confirming the oxidative conditions by extracellular ROS measurement. More detailed information can be found in the **Supporting Information**.

C2BBe1/HT29-MTX cell monolayer: cells were seeded on 12-Transwell cell culture inserts at a seeding density of 70,000 cells per cm^2 with C2BBe1 and HT29-MTX cells in a ratio of 9:1, the medium was replaced every other day until the cell monolayer was formed after 21 days. TEER was measured all over the 21 days to control the development of tight junctions.

Mucoadhesion of the particles to C2BBe1/HT29-MTX cell monolayers: Cell monolayers were washed with HBSS–HEPES, then 200 µL suspension of labelled particles in HBSS–HEPES (250 µg ml^{-1}) was added and incubated for 4 h at 37 °C. After incubation, the monolayerss were washed twice with HBSS–HEPES (pH 7.4) to remove the particles not attached and fixed with 4% paraformaldehyde at room temperature for 15 min. Wheat Germ Agglutinin-Alexa Fluor 594 conjugate (WGA-AF 594) (10 µg mL^{-1}) was incubated 10 minutes to stain the mucus. After washing, the Transwell filter was excised, embedded in a mounting medium containing DAPI and mounted on glass slides for confocal imaging. The particle–cell interactions were observed using CLSM (Leica SP5, Leica Microsystems, Germany).

Drug permeability across C2BBe1/HT29-MTX cell monolayer: The permeability of RIF across the cell monolayers was investigated from the apical (0.5 mL) to basolateral direction (1.5 mL) at 37 °C with shaking at 100 rpm. HBSS–HEPES buffer solution pH 7.4 was used in the received compartment, whereas HBSS–HEPES buffer (pH 6.8) with or without 1 mM of H_2O_2 was employed in the donor compartment to simulate healthy and oxidative extracellular medium conditions,

respectively. Samples were added on the apical part to have a final RIF concentration of 6 µg ml^{-1}. At specific time points (15, 30, 60, 90, 120 and 180 min) 100 µl of the release medium were withdrawn from the basolateral part and replaced with fresh medium. The amount of drug permeated in the basolateral compartment was quantified by HPLC and the P_{app} was calculated.[38] The experiments were carried out in triplicate.

Flat embedding TEM: After permeability studies, the cell monolayers were fixed with 2.5% glutaraldehyde (Sigma-Aldrich, USA) in 0.1 M of phosphate buffer saline (PBS) (pH 7.4) for 20 min at room temperature. Then, the wells were washed twice with sodium cacodylate buffer (NaCac) for 3 min. After that, the cell monolayers were post-fixed with 1% of osmium tetroxide in 0.1 M of NaCac buffer (pH 7.4) and then dehydrated and embedded in epoxy resin. Ultrathin sections (60 nm) were cut perpendicularly to the inserts, post-stained with uranyl acetate and lead citrate, and examined with TEM.

Statistical Analysis: All results were expressed as mean ± standard deviation (S.D.). Analysis of variance (ANOVA) followed by the Bonferroni post hoc test (GraphPadPrism, GraphPad software Inc., CA, USA) was used to analyse the data and the level of significance was set at the probabilities of $*p < 0.05$, $**p < 0.01$ and $***p < 0.001$.

Supporting Information

Supporting Information is available from the Wiley Online Library or from the author.

Acknowledgements

S.B. acknowledges the Department of Pharmacy and BioTechnology, University of Bologna, for the Marco Polo travel grant. Dr. W.L. acknowledges the Orion Research Foundation for financial support. Prof. H.A.S. acknowledges financial support from the Sigrid Juselius Foundation (Decision No. 4704580), the European Research Council under the European Union's Seventh Framework Programme (FP/2007-2013, Grant No. 310892), and the University of Helsinki and the HiLIFE Research Funds. The authors thank Prof. Bruno Sarmento (University of Porto, Portugal) for donating the cell line C2BBe1.

Received: ((will be filled in by the editorial staff))
Revised: ((will be filled in by the editorial staff))
Published online: ((will be filled in by the editorial staff))

References

[1] Q. Xu, C. He, C. Xiao, X. Chen, *Macromol. Biosci.* **2016**, *16*, 635.

[2] C.-C. Song, R. Ji, F.-S. Du, Z.-C. Li, *Macromolecules*, **2013**, *46*, 8416.

[3] C. de Gracia Lux, S. Joshi-Barr, T. Nguyen, E. Mahmoud, E. Schopf, N. Fomina, A. Almutairi, *J. Am. Chem. Soc.*, **2012**, *134*, 15758.

[4] a) D. Zhang, Y. Wei, K. Chen, X. Zhang, X. Xu, Q. Shi, S. Han, X. Chen, H. Gong, X. Li, J. Zhang, *Adv. Healthcare Mater.* **2015**, *4*, 69

b) Q. Zhang, F. Zhang, Y. Chen, Y. Dou, H. Tao, D. Zhang, R. Wang, X. Li, J. Zhang, *Chem. Mater.* **2017**, *29*, 8221

[5] F.-Y. Qiu, L. Yu, F.-S. Du, Z.-C. Li, *Macromol. Rapid Commun.* **2017**, *38*, 1700400

[6] T. Zhang, X. Chen, C. Xiao, X. Zhuang, X. Chen, *Polym. Chem.* **2017**, *8*, 6209

[7] K. E. Broaders, S. Grandhe, J. M. J. Fréchet, *J. Am. Chem. Soc.* **2011**, *133*, 756.

[8] B. Khor, A. Gardet, J. R. Xavier, *Nature* **2011**, *474*, 307.

[9] A. Maroni, L. Zema, M. D. Del Curto, A. Foppoli, A. Gazzaniga, *Adv. Drug Deliv. Rev.* **2012**, *64*, 540.

[10] N. J. Talley, M. T. Abreu, J. Achkar, C. N. Bernstein, M. C. Dubinsky, S. B. Hanauer, S. V. Kane, W. J. Sandborn, T. A. Ullman, P. Moayyedi, *Am. J. Gastroenterol*. **2011**, *106*, S2.

[11] G. Rogler, *Best Pract. Res. Clin. Gastroenterol.* **2010**, *24*, 157.

[12] Y. Yang, G. R. Lichtenstein, *Am. J. Gastroenterol.* **2002**, *97*, 803.

[13] T. Tian, Z. Wang, J. Zhang, *Oxid. Med. Cell. Longev.* **2017**, *2017*, 1.

[14] N. J. Simmonds, R. E. Allen, T. R. Stevens, R. N. Van Someren, D. R. Blake, D. S. Rampton, *Gastroenterology* **1992**, *103*, 188.

[15] L. Lih-Brody, S. R. Powell, K. P. Collier, G. M. Reddy, R. Cerchia, E. Kahn, G. S. Weissman, S. Katz, R. A. Floyd, M. J. McKinley, S. E. Fisher, G. E. Mullin, *Dig. Dis. Sci.* **1996**, *41*, 2078.

[16] D. S. Wilson, G. Dalmasso, L. Wang, S. V Sitaraman, D. Merlin, *Nat. Mater.* **2010**, *9*, 923.

[17] Q. Zhang, H. Tao, Y. Lin Y, Y. Hu, H. An, D. Zhang, S. Feng, H. Hu, R. Wang, X. Li, J. Zhang, *Biomaterials* **2016**, *105*, 206.

[18] A. Lamprecht, U. Scha, C.-M. Lehr, *Pharm. Res.* **2001**, *18*, 788.

[19] S. Hua, E. Marks, J. J. Schneider, S. Keely, *Nanomedicine: NBM* **2015**, *11*, 1117.

[20] R. B. Sartor, *Aliment. Pharmacol. Ther*. **2016**, *43*, 27.

[21] M. Guslandi, *World J. Gastroenterol.* **2011**, *17*, 4643.

[22] D. Liu, H. Zhang, B. Herranz-Blanco, E. Mäkilä, V.-P. Lehto, J. Salonen, J. Hirvonen, H. A. Santos, *Small* **2014**, *10*, 2029

[23] D. Liu, H. Zhang, S. Cito, J. Fan, J. Salonen, J. Hirvonen, T. M. Sikanen, D. A. Weitz, *Nano Lett.* **2017**, *17*, 606.

[24] X. Li, J. Zhu, Z. Man, Y. Ao, H. Chen, R. Yb, *Sci. Rep.* **2014**, *4*, 1.

[25] a) X. Lin, P. Han, S. Dong, H. Li, *RSC Adv.* **2015**, *5*, 69886. b) M. G. Sankalia, R. C. Mashru, J. M. Sankalia, V. B. Sutariya, *Eur. J. Pharm. Biopharm.* **2007**, *65*, 215.

[26] H. S. Mansur, A. A. P. Mansur, E. Curti, M. V De Almeida, *J. Mater. Chem. B* **2013**, *1*, 1696.

[27] a) S. R. Inglis, E. C. Y. Woon, A. L. Thompson, C. J. Schofield, *J. Org. Chem.* **2010**, *75*, 468. b) J. Sun, M. T. Perfetti, W. L. Santos, *J Org Chem*. **2011**, *76*, 3571.

[28] N. Kerdsakundee, W. Li, J. P. Martins, Z. Liu, F. Zhang, M. Kemell, A. Correia, Y. Ding, M. Airavaara, J. Hirvonen, R. Wiwattanapatapee, H. A. Santos, *Adv. Healthc. Mater.* **2017**, *6*, 1.

[29] F. Araújo, B. Sarmento, *Int. J. Pharm.* **2013**, *458*, 128.

[30] S. A. Ingersoll, S. Ayyadurai, M. A. Charania, H. Laroui, Y. Yan, D. Merlin, *Am. J. Physiol. - Gastrointest. Liver Physiol.* **2012**, *302*, G484.

[31] M. E. V Johansson, H. Sjövall, G. C. Hansson, *Nat. Rev. Gastroenterol. Hepatol.* **2013**, *10*, 352.

[32] F. Leonard, E. Collnot, C. Lehr, *Mol. Pharm.* **2010**, *7*, 2103.

[33] I. A. Sogias, A. C. Williams, V. V. Khutoryanskiy, *Biomacromolecules* **2008**, *9*, 1837.

[34] E. Walter, S. Janich, B. J. Roessler, J. M. Hilfinger, G. L. Amidon, *J. Pharm. Sci.* **1996**, *85*, 1070.

[35] T. Hidalgo, E. Bellido, J. Avila, M. C. Asensio, F. Salles, M. V. Lozano, M. Guillevic, R. Simón-Vázquez, A. González-Fernández, C. Serre, M. J. Alonso, P. Horcajada, *Sci. Rep.* **2017**, *3*, 1.

[36] R. Coco, L. Plapied, V. Pourcelle, C. Jérôme, D. J. Brayden, Y. J. Schneider, V. Préat, *Int. J. Pharm.* **2013**, *440*, 3.

[37] W. Li, D. Liu, H. Zhang, A. Correia, E. Mäkilä, J. Salonen, J. Hirvonen, H. A. Santos, *Acta Biomater.* **2017**, *48*, 238.

[38] D. Liu, L. M. Bimbo, E. Mäkilä, F. Villanova, M. Kaasalainen, *J. Control. Release* **2013**, *170*, 268.

An advanced nano-in-micro composite is successfully prepared with a phenylboronic esters-modified dextran (OxiDEX) to achieve an oxidation-responsive drug delivery for the therapy of inflammatory bowel disease. H_2O_2-selective OxiDEX degradation and consequent drug release are demonstrated. The composite limits the drug permeation through intestinal epithelium providing a promising approach to limit unspecific absorption and systemic side effects.

Inflammatory bowel disease, ROS-responsive, oxidation-responsive, nanoparticles, microfluidics

S. Bertoni, Z. Liu, A. Correia, J. P. Martins, Dr. A. Rahikkala, F. Fontana, M. Kemell, Dongfei Liu, B. Albertini, N. Passerini*, W. Li*, H. A. Santos*

Reactive oxygen species-responsive nano-in-micro composite for targeted therapy of inflammatory bowel disease

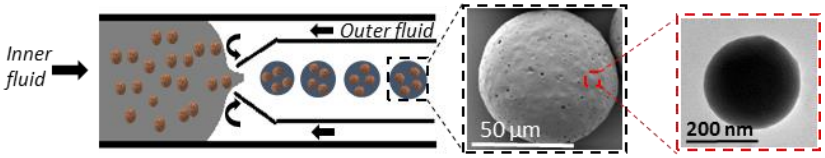

Supporting Information

Reactive oxygen species-responsive nano-in-micro composite for targeted therapy of inflammatory bowel disease

Serena Bertoni, Zehua Liu, Alexandra Correia, João Pedro Martins, Antti Rahikkala, Flavia Fontana, Marianna Kemell, Dongfei Liu, Beatrice Albertini, Nadia Passerini, Wei Li*, Hélder A. Santos**

S. Bertoni, Dr. W. Li, Z. Liu, A. Correia, J. P. Martins, Dr. A. Rahikkala, F. Fontana, Dr. D. Liu, Prof. H. A. Santos
Drug Research Program, Division of Pharmaceutical Chemistry and Technology, Faculty of Pharmacy, University of Helsinki, Helsinki 00014, Finland
E-mail: wei.li@helsinki.fi, helder.santos@helsinki.fi

Dr. D. Liu, Prof. H. A. Santos
Helsinki Institute of Life Science (HiLIFE), University of Helsinki
Helsinki 00014, Finland

S. Bertoni, Prof. B. Albertini, Prof. N. Passerini
PharmTech Lab, Department of Pharmacy and BioTechnology, University of Bologna, Via S. Donato 19/2, Bologna 40127, Italy
E-mail: nadia.passerini@unibo.it

Dr. M. Kemell
Department of Chemistry, University of Helsinki, Helsinki 00014, Finland

Experimental section

Synthesis of OxiDEX: Briefly, 4-(Hydroxymethyl)-phenylboronic acid pinacol ester (PAPE) (4 g, 17.1 mmol) was dissolved in dry dichloromethane (CH_2Cl_2) (20 ml) in a dried 200 ml flask. Carbonyldiimidazole (5.54 g, 34.2 mmol) was then added to the solution and stirred for 1 h. The mixture was concentrated under vacuum, redissolved in ethyl acetate (200 ml) and washed with H_2O (3 × 10 mL). The organics were dried with $MgSO_4$, and concentrated using a rotary evaporator to give 4-(Imidazoyl carbamate)phenylboronic acid pinacol ester. The as-prepared product (0.5 g, 2.5 mmol) was added to 1 mL of DMSO, afterwards 90 mg of dextran (Mw= 9000-11000 Da, Sigma Aldrich, USA) was dissolved in the solution followed by DMAP (0.18 g, 7.5 mmol) addition, and the mixture solution was stirred overnight at 40 ℃ to yield the final product. After the reaction, extra water was added to precipitate out the polymer, the polymer was washed with water for 3 times and lyophilized.

Study of cell monolayers in oxidative conditions: Cell monolayers at day 21 were washed twice with HBSS–HEPES buffer solution (pH 7.4). Then, monolayers were incubated 24 h with HBSS–HEPES and with a cocktail of IL-1β (20 ng ml^{-1}) and H_2O_2 (0.05 mM) in HBSS–HEPES buffer for healthy and oxidative conditions, respectively. After 24 h incubation, the buffer was removed from the upper and basolateral compartment and monolayers used for membrane integrity and mucin determination.

Extracellular ROS: 2′,7′-dichlorofluorescin diacetate (DCFH-DA, Sigma Aldrich) method was used with modifications to detect extracellular ROS. Briefly, DCFH-DA was deacetylated to DCFH *in vitro* by addition of 20 mM NaOH;[1] the modification was done to make the molecule hydrophilic and prevent it to cross the cell membrane. DCFH was added to 100 µl of the cell buffer at a concentration of 10 µg ml^{-1} and the amount of the oxidized fluorescent 2',7'-dichlorofluorescein

(DCF) was detected by using a Varioskan Flash plate reader (Thermo Fisher Scientific, USA) with an excitation wavelength and an emission wavelength of 488 nm and 522 nm, respectively.

Membrane integrity: For the membrane integrity, TEER measurement were carried out using Millicell-Electrical Resistance System (Millipore, USA).

Mucus layer amount and distribution: The content of the main mucus glycoprotein mucin in cell buffer (extracellular mucin content) and after cell lysis (intracellular mucin content) was quantified using the periodic acid/Schiff reagent method as described previously.[2] After removing the cell buffer from the monolayers, cells were detached from the insert membrane, dispersed in 0.5 ml of HBSS–HEPES buffer and lysed by sonication (30 amplitude, 10 s) to release the mucin contained in the intracellular vesicles. Cell lysates were centrifuged and the supernatant was used to measure mucin content. Samples of cell buffer and cell lysate supernatant were then incubated at 37 °C for 2 h with 10 µL of periodic acid solution, which was prepared by diluting 0.5% of periodic acid solution (Sigma Aldrich) to 0.1% with 7% acetic acid. Afterwards, 20 µL of Schiff reagent (Sigma Aldrich) was added and samples were incubated at room temperature for 30 min before measuring absorption at 555 nm using Varioskan Flash plate reader (Thermo Fisher Scientific, USA). A calibration curve with a linear range of 5–500 µg ml^{-1} was generated using porcine mucin.

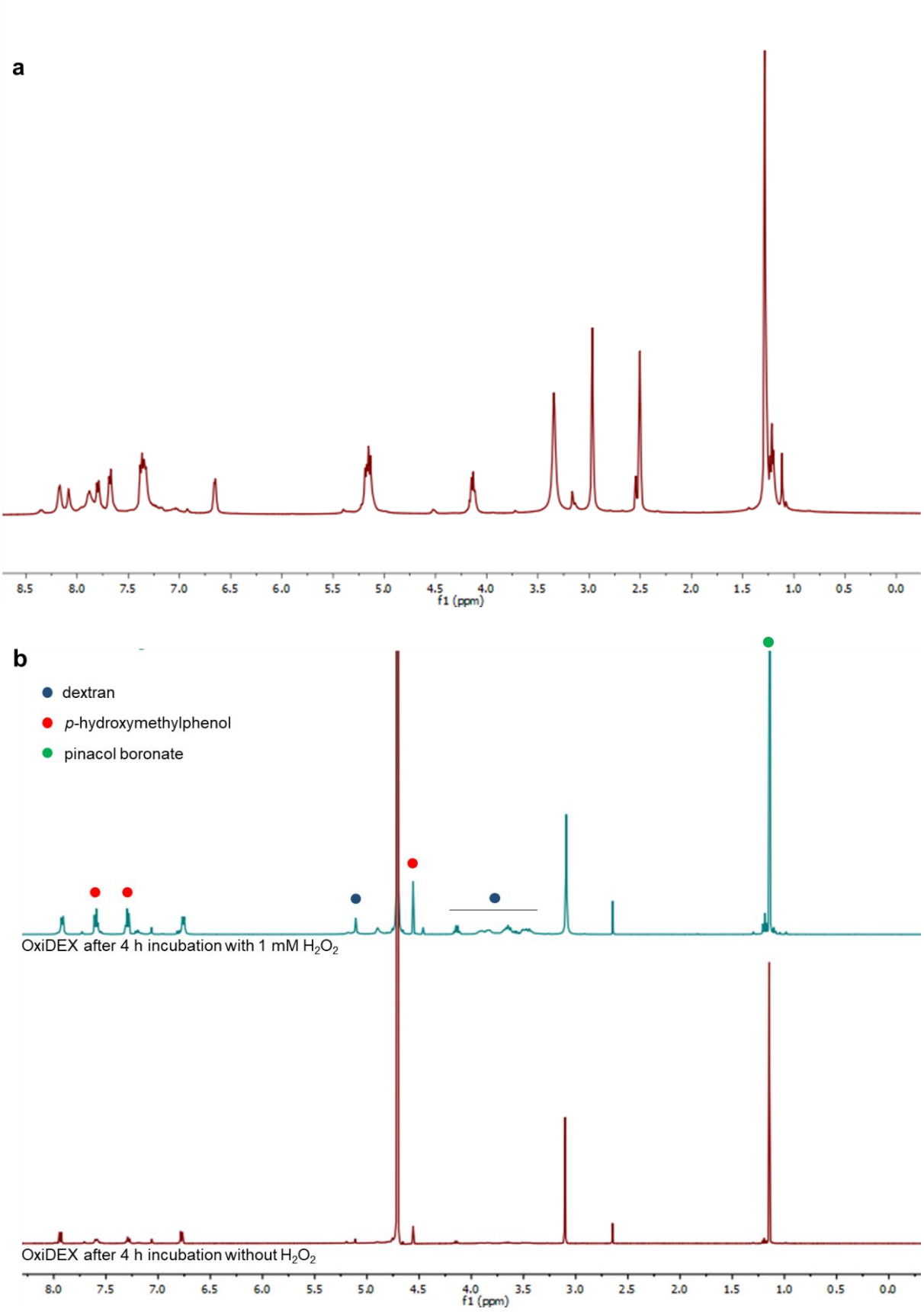

Figure S1. (a) ^{1}H NMR (400 MHz, DMSO-*d6*) spectrum of OxiDEX polymer. Characteristic peaks of the phenyl boronic ester group can be seen at δ 1.21 (s, 12 H, -CH3) and in the aromatic area at δ 7.35 (d, 2 H, Ar H) and δ 7.60 (d, 2 H, Ar H). (b) ^{1}H NMR (400 MHz, D_2O) spectrum of OxiDEX polymer after 4 h treatment with or without 1 mM H_2O_2. Appearance of *p*-hydroxymethylphenol (characteristics peaks at δ 4.56 and in the aromatic area at δ 7.29 and δ 7.59), dextran (characteristics peaks at δ 3.42-4.17 and at δ 5.11), and pinacol boronate (characteristics peak at δ 3.09) can be observed.

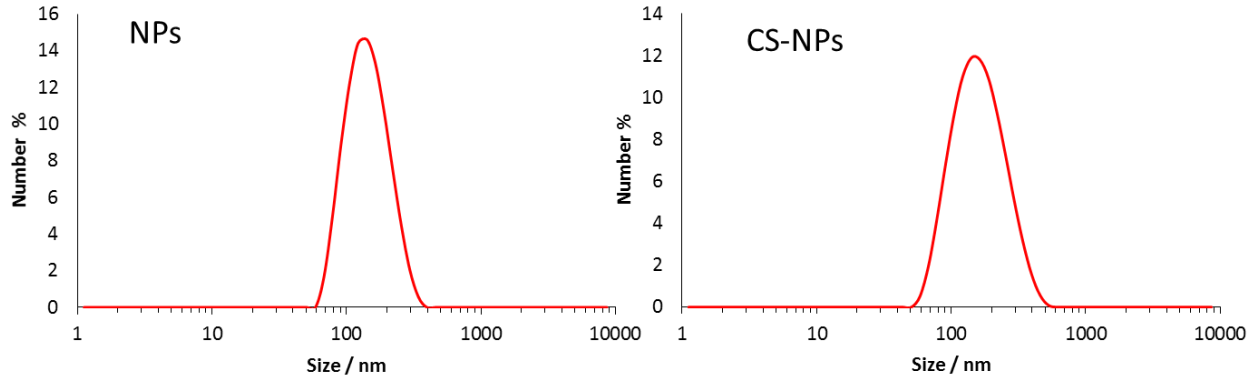

Figure S2. Example of particle size distribution of NPs and CS-NPs measured by DLS.

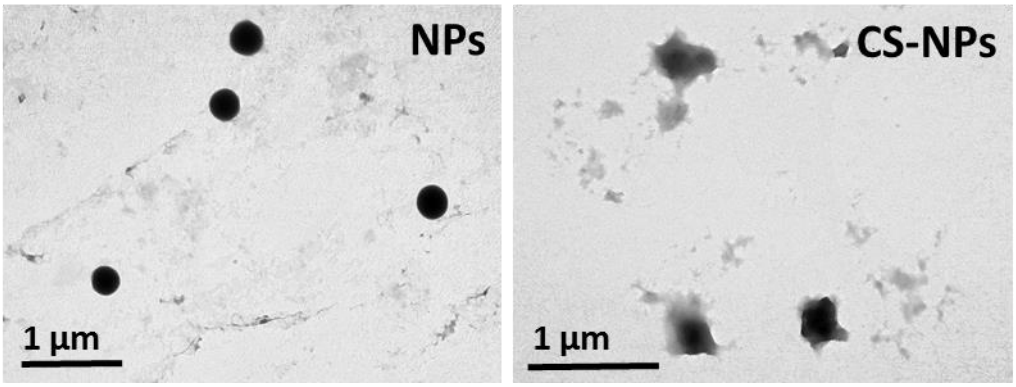

Figure S3. TEM images of NPs and CS-NPs.

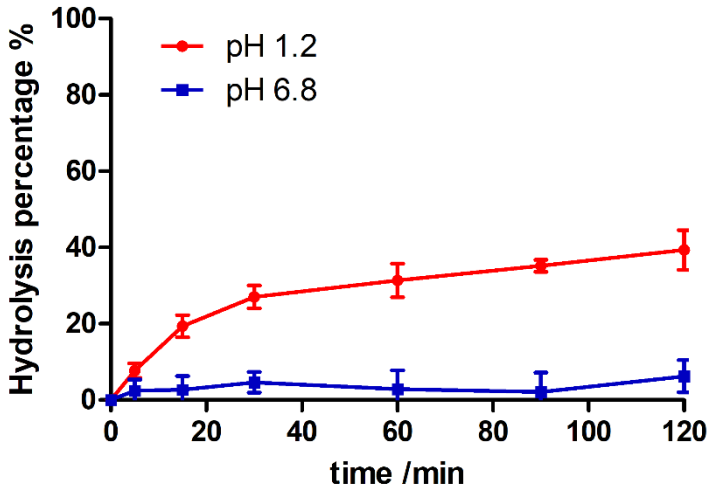

Figure S4. Hydrolysis profiles of OxiDEX NPs in various GI tract pH conditions: SGF at pH 1.2 and PBS at pH 6.8.

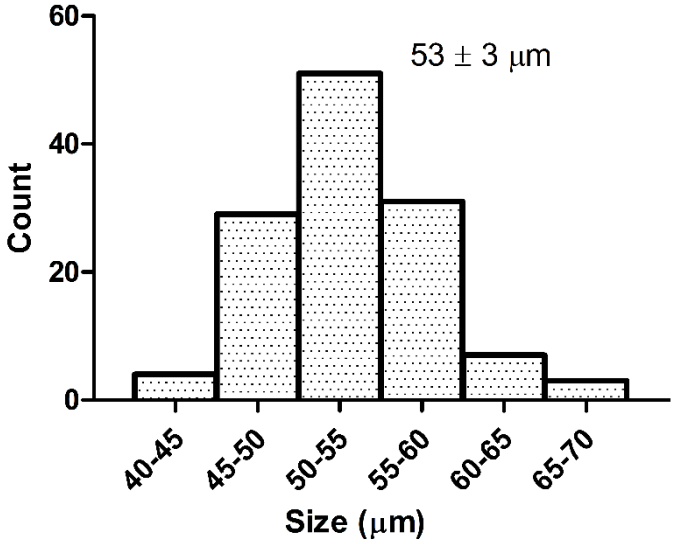

Figure S5. Particle size distribution of NPs@MF composites.

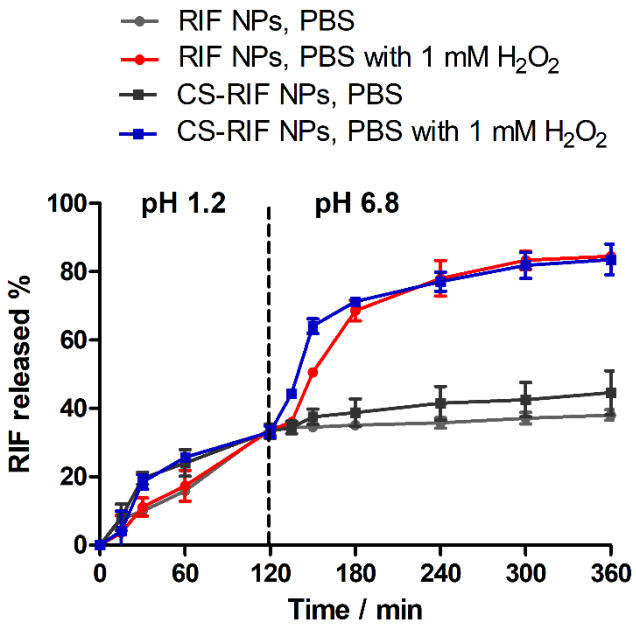

Figure S6. Drug release profiles of nanoparticles (RIF NPs and CS-RIF NPs) first in SGF (pH 1.2) for 2 h and then in PBS (pH 6.8) with or without H_2O_2 for 6 h. Data represent mean ± S.D. (n = 3).

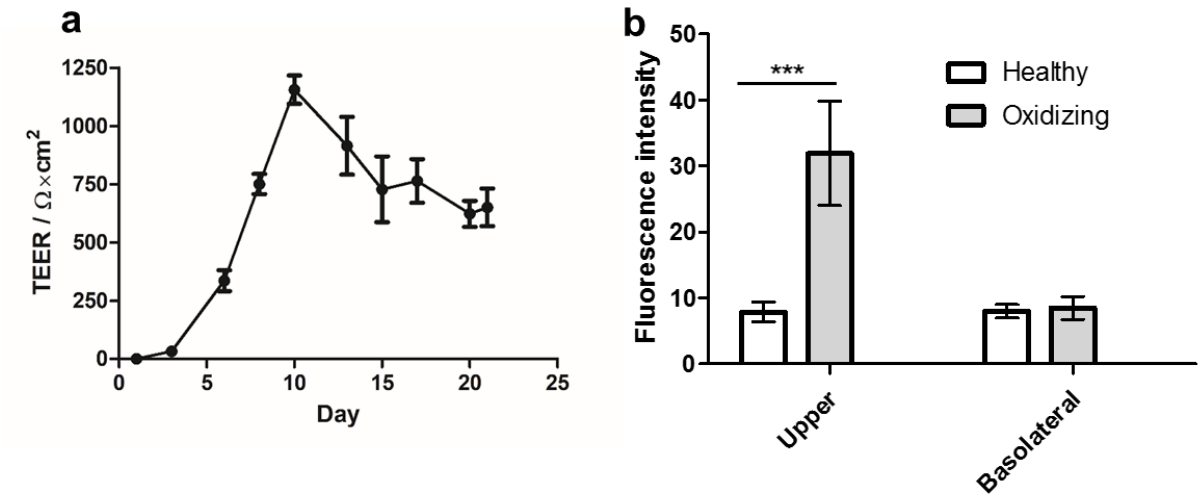

Figure S7. (a) TEER changes during the 21 days of co-cultured C2BBe1/HT29-MTX (ratio of 9:1) cell monolayers. (b) Extracellular ROS measurement in upper and basolateral medium from cell monolayers in healthy and oxidizing conditions. For oxidizing conditions, monolayers were treated

with 20 ng ml^{-1} of IL-1β and 50 μM of H_2O_2 for 24 h. The level of significance was set at the probability of ***$p < 0.001$.

References

[1] K. Hafer, K. S. Iwamoto, R. H. Schiestl, *Radiat. Res.* **2008**, *169*, 460.

[2] F. Leonard, E. Collnot, C. Lehr, *Mol. Pharm.* **2010**, *7*, 2103.